



ELSEVIER

Physica A 231 (1996) 425–438

PHYSICA A

174

Equilibrium and nonequilibrium thermomechanics for an effective pair potential used in smooth particle applied mechanics

Wm.G. Hoover^{a,*}, Siegfried Hess^b

^a *University of California at Davis / Livermore and Lawrence Livermore National Laboratory,
Livermore, CA 94551-7808, USA*

^b *Institute for Theoretical Physics, Technical University Berlin, Hardenbergstrasse 36,
D-10623 Berlin, Germany*

Received 29 April 1996

Abstract

The smooth-particle weighting functions used in numerical solutions of the thermo-mechanical continuum equations can be interpreted as weak pair potentials from the standpoint of statistical physics. We examine both equilibrium and nonequilibrium thermomechanical properties of many-body systems using a typical smooth particle potential, Lucy's, and discuss the implications for macroscopic continuum simulations.

PACS: 05.20.Dd; 07.05.Tp; 66.20. + d; 67.55.Hc

1. Introduction

Smooth particle applied mechanics was invented, simultaneously and independently, by Lucy and Monaghan, in 1977 [1]. It is a particle method for solving the continuum equations, with the particles playing the role of moving grid points. The accelerations and trajectories of these particles depend upon the form of the underlying continuum constitutive relations. We speak of the “invention” of the smooth particle method, rather than its “discovery”, simply because it incorporates many arbitrary features. The smooth particle method represents *all* the field variables of continuum mechanics, including density, velocity, and energy, as sums of individual particle contributions. The range associated with these contributions, h , and the form of the weighting function $w(r)$, are chosen arbitrarily, but typically in such a way that 20 or 30 “smooth particles” contribute to the values of the continuum field variables $\{\rho, v, e\}$ at a particular location. There is, in addition, some representational arbitrariness in the spatial average of the continuum equations as motion equations for the representative

*Corresponding author. Fax: 510-422-8681; e-mail: hoover@wente.llnl.gov.

smooth particles. It is a symptom of this arbitrariness that the particles have individual velocities and energies $\{v, e\}_i$ which differ from the field quantities $\langle v \rangle$ and $\langle e \rangle$ at the locations of these same particles. Generally, the smoothed averaged quantities display smaller fluctuations, and hence are more continuum-like, than the individual particle quantities.

The most common form of the equation of motion for the smooth particles is

$$m\dot{v}_i = -m^2 \sum [(P/\rho^2)_i + (P/\rho^2)_j] \cdot \nabla_i w(r_{ij}), \quad (1)$$

where the pressure tensors for particles i and j can depend on the velocity gradients in their vicinity,

$$(\nabla v)_i = m \sum [v_k - v_i] (1/\rho_{ik}) \cdot \nabla_i w(r_{ik}), \quad (2)$$

where ρ_{ik} is the arithmetic or geometric mean of ρ_i and ρ_k , and where, for simplicity, we take all the individual particle masses to have a common value, m . The individual particle densities in Eqs. (1) and (2) are sums of contributions from nearby particles, including the particle in question:

$$\rho_i \equiv m \sum w(r_{ij}).$$

The main advantage of the motion equation (1) relative to some alternatives is that it conserves momentum exactly, due to the antisymmetry of the ∇w contributions to interacting pairs of particles. When the pressure tensor is anisotropic this approach does not necessarily conserve angular momentum.

Smooth particle simulation has been applied to a variety of astrophysical problems as well as to problems in conventional solid and fluid mechanics [2–5]. The somewhat arbitrary nature of the approach suggests that it is useful to take up a host of interesting related problems in statistical mechanics, both at and away from equilibrium, so as to understand the method better. The simplest physical application of smooth particle applied mechanics corresponds to the adiabatic isentropic deformation of a two-dimensional ideal gas, with a scalar pressure $P \propto \rho^2$, for which the continuum equation of motion (1) reduces to the ordinary atomistic equation of motion for molecular dynamics,

$$m\dot{v}_i = -\sum \nabla_i w_{ij} = -\sum \nabla_i \phi_{ij}, \quad (3)$$

with $w(r) \equiv \phi(r)$ playing the role of a pair potential. For other equations of state, smooth particle dynamics is not precisely isomorphic to molecular dynamics. But, whenever the pressure and density are approximately constant – as at equilibrium, for example – the smooth particles representing a continuum resemble particles obeying the motion equations of conventional molecular dynamics. It is for this reason that we consider here the properties of a typical weighting function, Lucy's, viewed as a pair potential. This choice,

$$w_{\text{LUCY}} = \begin{cases} (5/\pi h^2) [1 + (3r/h)] [1 - (r/h)]^3, & r \leq h, \\ 0, & r > h, \end{cases}$$

has continuous first and second derivatives, which facilitates accurate numerical integration of the motion equations. The proportionality constant is determined in such a way that the D -dimensional integral of w is unity, so that the two-dimensional value ($5/\pi h^2$) is replaced by ($105/16\pi h^3$) in three dimensions. Gross properties of the Lucy potential should resemble those of a repulsive Gaussian potential, for which a similar normalization would be expressed in terms of the Gaussian function's halfwidth.

For particle simulations it is advantageous to use a potential of the shortest possible range. Throughout this paper we set the "range" of the weighting function equal to unity, for convenience. A principle of corresponding states holds which allows all the equilibrium and nonequilibrium properties for other values of the range to be expressed in terms of those for $h = 1$. The next section is devoted to a discussion of this principle. The following sections are devoted to the discussion of time reversibility, thermodynamic, and hydrodynamic properties of Lucy's potential. The final section is a summary in which applications to continuum simulations are stressed.

2. Corresponding states principle for smooth particles

The dynamics of any configuration of smooth particles, at locations $\{r\}$, with velocities $\{v\}$, energies per unit mass $\{e\}$, and with a weighting function of range h , can alternatively be viewed in a scaled space, with a weighting function of unit range. It is this scaled-space choice that we adopt here in our numerical work. In the scaled space both the distances and the velocities are decreased by a factor h , so that h is replaced by unity. The normalized weighting function is thereby *increased* by a factor h^D , where D is the dimensionality of the space, usually 2 or 3. The dynamics of the original configuration is thus replaced by a scaled dynamics. This scaled dynamics is a faithful model of the original provided that the kinetic energy in the scaled system is also increased by a factor of h^D . This can be achieved by scaling the mass or the time. For simplicity, we adopt a universal scale-independent time, and choose mass scaling, requiring that the stronger forces in the high-density system are applied to more massive bodies, more massive by a factor of h^{2+D} in D dimensions.

These choices allow the *same* time scale to be used in both systems while maintaining also the same ratio of kinetic to potential energy. Any of the physical properties of the scaled system ($h = 1$) can then be expressed in terms of those for the original system. Dimensionless properties, such as PV/NkT , E/NkT , or Reynolds' number, are necessarily identical in the two systems.

To illustrate, consider the scaling of energy for a two-dimensional system with $h = 3$ and $N/V = 1$. This corresponds, in the scaled space emphasized in this paper, with $h = 1$, to a number density of $h^D = 3^2 = 9$. Knowing $E = K + \Phi$ in the original system gives $E_{\text{SCALED}} = 9E$. In the kinetic energy the velocities are reduced by a factor 3, while the mass increased by a factor 81, giving an overall increase in kinetic energy of a factor $81/3^2 = 9$. Another energy, PV , scales in the same way. The hydrodynamic

Table 1

Scaling relationships illustrating the corresponding states principle linking thermomechanical properties for the h -dependent Lucy potential to higher-density properties for a standard potential with characteristic length $h = 1$. Here we tabulate the ratio of each quantity in a system with smoothing length h to the same quantity in a higher-density system with $h = 1$

Time: h^0	Length: h	Velocity: h
Force: h^{-D-1}	Energy (K): h^{-D}	Energy (Φ): h^{-D}
Mass: h^{-D-2}	Volume: h^D	Stress: h^{-2D}
Temperature: h^{-D}	Viscosity: h^{-2D}	

transport coefficients, kinematic viscosity ν and thermal diffusivity D^T , are proportional to the squares of lengths. Thus,

$$\nu_1 = \nu_h/h^2 = (\eta/\rho)_h/h^2; \quad D_1^T \equiv (\kappa/\rho c_v)_1 = (\kappa/\rho c_v)_h/h^2,$$

where η is the shear viscosity, ρ is the mass density, κ is the thermal conductivity and c_v is the heat capacity per unit mass, $\frac{1}{2}Dk$ for a D -dimensional ideal gas, for instance. Table 1 summarizes a selection of such scaling properties. This corresponding states principle is similar to that which holds for the Lennard-Jones potential and for the family of inverse power potentials, as is discussed at length in the treatise of Hirschfelder et al. [6].

3. Turbulence, time reversibility, and the Lucy potential

Theoretical discussions of turbulence often center on an idealized situation in which ordinary molecular viscous dissipation and conductive heat transfer are both absent. The corresponding ideal fluid is called an ‘‘Euler fluid’’ because it obeys the Eulerian equations of fluid mechanics, in which the viscosities and the thermal diffusivity do not appear. If it is true that such a limiting case can be realized in numerical simulations, the model should be a prototypical basis for theoretical analyses of turbulent flows. If instead the limiting case is not well defined then alternative attempts to describe it computationally will lack consistency with one another. This potential application, as a basis for studying turbulence, recommends the investigation of smooth particles as a model for the Euler fluid. One would expect such a model to display a statistical distribution of eddy-current kinetic energies resembling that of a real fluid at high Reynolds number. An attempt to carry out such a set of simulations, with smooth particles, was not definitive [5]. Better agreement with Kolmogorov’s $k^{-5/3}$ eddy-current energy spectrum was achieved in a small 1024-particle system than in a system four times larger.

The Lucy potential model has some independent interest from the standpoint of time reversibility. Boltzmann’s explanation of irreversible behaviour in gases, based on the Boltzmann equation, still retains an air of paradox and contradiction over

a century later. It has recently been pointed out that the use of Lucy's potential to model the dynamics of an Euler fluid (with neither viscosity nor heat conductivity) provides an inverted version of Boltzmann's reversibility paradox [7]. The fluid being represented, since it lacks transport coefficients, can display no dissipation. On the other hand, the representation of this fluid by ordinary molecular dynamics, using Lucy's potential function, implies the existence of intrinsic transport coefficients, as given by the Boltzmann equation at low density, and by the Green–Kubo theory at any density.

Applications, to turbulence and to a deeper understanding of Boltzmann's paradox, provide additional motivation for studying the Lucy model. A further motivation, noted but not yet pursued, is the understanding of a peculiar shear-flow instability, in which a single particle came to possess most of the system kinetic energy [3]. All of these problems are fertile ground for further research. For this reason we study here some of the most basic properties of the Lucy model, the mechanical and thermal equations of state and the low-density linear transport coefficients. Our results are described in the next two sections.

4. Thermodynamic equilibrium properties of the Lucy fluid

At low temperatures the Lucy potential can exist in an amazing variety of crystal-line structures. Because the potential has no repulsive hard core there is no maximum density. Thus there is a bewildering variety of phase transformations as the cold material is compressed from low density to high, with the high-density limit approached in a peculiar way, with each lattice site occupied by sufficiently many particles that neighboring particles are at least unit distance (for $h = 1$) apart. The stabilities of the various crystal structures can be investigated in terms of the elastic moduli [8] or, more simply, by inspection of a simulation carried out with damping sufficient to slowly extract all the kinetic energy. We ignore solid-phase properties in the present work but emphasize their intrinsic interest as another open research area.

Because the Lucy potential is primarily of interest as a model for fluids we have determined an accurate fluid-phase equation of state for it, varying density, pressure, temperature, and energy over wide ranges. These data were generated by straightforward isoenergetic and isokinetic molecular dynamics simulations [9]. A fast work station can easily provide mechanical and thermal equations of state, to three-figure accuracy at hundreds of state points. Representative data are displayed in Tables 2 and 3. For the convenience of the reader we have provided two sets of data, the first giving pressure and temperature as functions of energy and volume, as is the usual hydrodynamic practice, and the second giving pressure and energy as functions of temperature and volume, as is the usual practice in statistical mechanics. The isothermal simulations were performed at constant (kinetic) temperature by imposing a constraint on the total kinetic energy of the isothermal systems [10]. At the level of accuracy shown in the tables there is no difference between simulations with 100, 256,

Table 2

Selected values of the energy and pressure-volume product for the Lucy potential. The results are given as sums of the potential and kinetic parts. Corresponding values for $h \neq 1$ can be derived by using the scaling relationships described in the text. Note that the kinetic contributions to the energy per particle and to PV/N are identical. All the simulations were carried out with periodic boundaries, using the fourth-order Runge-Kutta method with a time step of 0.02, rescaling the velocities as needed to retain 12-digit accuracy in the total energy

$E/N:$			
$\rho = 1$	$\rho = 4$	$\rho = 7$	$\rho = 10$
0.16 + 0.34	1.44 + 0.56	2.88 + 0.62	4.35 + 0.65
0.34 + 1.66	1.63 + 1.87	3.03 + 1.97	4.48 + 2.02
0.40 + 3.10	1.72 + 3.28	3.13 + 3.38	4.56 + 3.44
0.42 + 4.58	1.77 + 4.73	3.18 + 4.82	4.62 + 4.88
$PV/N:$			
$\rho = 1$	$\rho = 4$	$\rho = 7$	$\rho = 10$
0.32 + 0.34	1.83 + 0.56	3.35 + 0.62	4.86 + 0.65
0.42 + 1.66	1.85 + 1.87	3.34 + 1.97	4.83 + 2.02
0.45 + 3.10	1.87 + 3.28	3.35 + 3.38	4.84 + 3.44
0.46 + 4.58	1.89 + 4.73	3.36 + 4.82	4.84 + 4.88

Table 3

Selected values of the energy and pressure-volume product for the Lucy potential. These are given as sums of the potential and kinetic parts. Corresponding values for $h \neq 1$ can be derived by using the scaling relationships described in the text. Note that the kinetic contributions to the energy per particle and to PV/N are identical. All the simulations were carried out with periodic boundaries, using the fourth-order Runge-Kutta method with a time step of 0.02, rescaling the velocities as needed to retain 12-digit accuracy in the kinetic energy

$E/N:$			
$\rho = 1$	$\rho = 4$	$\rho = 7$	$\rho = 10$
0.20 + 0.50	1.43 + 0.50	2.86 + 0.50	4.32 + 0.50
0.41 + 3.50	1.73 + 3.50	3.13 + 3.50	4.57 + 3.50
0.44 + 6.50	1.81 + 6.50	3.23 + 6.50	4.66 + 6.50
0.46 + 9.50	1.85 + 9.50	3.28 + 9.50	4.72 + 9.50
$PV/N:$			
$\rho = 1$	$\rho = 4$	$\rho = 7$	$\rho = 10$
0.35 + 0.50	1.84 + 0.50	3.36 + 0.50	4.87 + 0.50
0.45 + 3.50	1.88 + 3.50	3.35 + 3.50	4.84 + 3.50
0.47 + 6.50	1.91 + 6.50	3.37 + 6.50	4.85 + 6.50
0.48 + 9.50	1.92 + 9.50	3.39 + 9.50	4.87 + 9.50

or 1024 particles. We include not only the number density unity, for comparison with the usual statistical-mechanical theories of dense matter, but also densities severalfold greater, corresponding to the degree of packing useful in continuum simulations using smooth particle methods.

The results provide estimates of the potential contribution to the pressure and the energy accurate within about 1% over the whole range. The data can be summarized

as following very well the Grueneisen description, with the pressure, at constant volume, varying nearly linearly with energy. This should not be entirely surprising, for the high-density limit of the Lucy particles must furnish an exact representation of the underlying two-dimensional ideal-gas isentrope,

$$P = \rho e \propto \rho^2.$$

Likewise, the isochoric relation between temperature and energy is nearly linear. Further, both variations are almost density independent within the range spanned by the tables:

$$(\Delta PV/\Delta E)_v = 0.96; \quad (\Delta K/\Delta E)_v = Nk(\Delta T/\Delta E)_v = 0.93.$$

In order to see whether these small deviations from the ideal-gas equation of state can be simply understood on the basis of the Mayer's virial series [6], we have computed the temperature-dependent second virial coefficient B_2 and estimated the third B_3 in the virial expansion

$$PV/NkT = 1 + B_2(N/V) + B_3(N/V)^2 + \dots$$

Fig. 1 shows the degree to which this classic approach accounts for the collective smooth particle effects at the relatively high densities used in continuum simulations.

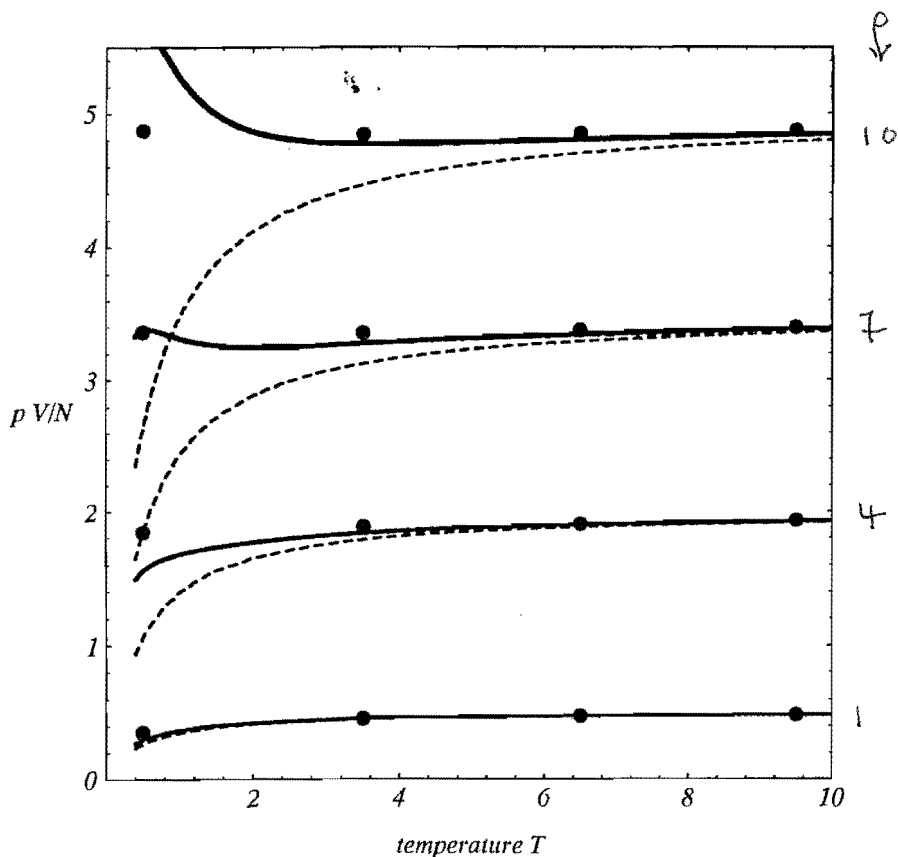


Fig. 1. Potential contribution to the smooth particle equation of state (points) compared to the predictions of the two- and three-term virial series (dashed and solid lines, respectively).

Despite the overall simplicity of the results, there are some surprises in the small details. At the higher number densities typical of smooth particle simulations, $Nh^D/V = 5$ and above, there is a definite decrease in thermal pressure with temperature. That is, the potential contribution to the pressure actually falls while the kinetic part doubles or triples in size. Such behavior is quite unlike that characterizing the usual short-ranged potentials used in computer simulations.

5. Kinetic and hydrodynamic properties for two-dimensional fluids

When the smooth particle method is used to model hydrodynamic flows in which viscosity has a noticeable influence, it is essential that any intrinsic artificial or numerical viscosity, stemming from the method itself, be considerably smaller than the true viscosity of the fluid being modelled. This requirement is sufficient motivation for a thorough study of the viscous response of the Lucy potential to shear.

Detailed computer simulations [9] of high-density viscous flow, for two different temperatures, and over a wide range of strain rates, showed strong temperature- and rate-dependences for the intrinsic Lucy-potential viscosity [3]. These simulations indicated a 20-fold increase in shear viscosity in response to an 8-fold isochoric temperature increase, consistent with an estimated temperature dependence $T^{3/2}$. The numerical viscosity values were in rough agreement with theoretical estimates.

Another very smooth potential function [11], resembling Lucy's in shape, and also used in two-dimensional shear-viscosity simulations [9],

$$\phi = \varepsilon[1 - (r/\sigma)^2]^4,$$

becomes a smooth particle weight function very much like Lucy's if ε is chosen to be $5/\pi h^2$ and σ is taken to be the range of the smoothing function, h . At a relatively low density for smooth particles, $Nh^2/V = 1$, the computed shear viscosities for this smooth potential agreed fairly well with estimates from Enskog's theory [6, 12–14].

The Enskog theory of dense-fluid transport is a natural starting point for estimating transport coefficients [6, 12–14]. That theory begins by introducing an equivalent hard-particle model of the fluid to be described. In the two-dimensional case hard disks are used. The size of the disks is estimated by matching the "thermal pressure" $T(\partial P/\partial T)_v$ to the disks' pressure. In the case of Lucy's potential our equilibrium computer simulations have established that the pressure is nearly ideal. In this case the Enskog theory suggests (perhaps incorrectly) that the *low density* kinetic-theory viscosity should be a good *high-density* estimate. An investigation of the two-dimensional heat conductivity for hard disks has recently been carried out [12], showing small deviations from Enskog's predictions.

We have used three different methods, all based on Boltzmann's equation, to evaluate the limiting low-density shear viscosity for the Lucy potential:

1. Numerical integration in terms of the scattering angle χ .
2. Numerical solution of the equilibrium Boltzmann equation.
3. Numerical solution of the nonequilibrium Boltzmann equation.

The first of these approaches is based on the conventional evaluation of the energy and impact-parameter dependence of the scattering angle χ , followed by an integration over the equilibrium velocity distribution. The required integral for the lowest-order contribution to the viscosity coefficient has the form:

$$\eta \equiv P/\omega_\eta;$$

$$\omega_\eta = 2(N/V)(kT/m)^{1/2} \int \gamma^6 \exp(-\gamma^2) d\gamma \int \sin^2 \chi db.$$

Here, γ is the relative velocity in units of $2(kT/m)^{1/2}$. We reproduce the more familiar three-dimensional expression solely for comparison [6, 14]:

$$\omega_\eta = \frac{16}{5} (N/V)(\pi kT/m)^{1/2} \int \gamma^7 \exp(-\gamma^2) d\gamma \int \sin^2 \chi b db.$$

At low temperature our numerical evaluations reproduce the first term in Sengers' more complete evaluation of the hard-disk result [13]:

$$\eta_{\text{COLD}} = \eta_{\text{DISK}} = 0.24(mkT)^{1/2}/h.$$

At high temperature the scattering angle is reduced, and ultimately varies as the ratio of potential to kinetic energy. The approach to that limit is clearly shown in Fig. 2, and leads to the high-temperature result:

$$\eta_{\text{HOT}} = 0.94(mkT)^{1/2}(kTh^2)^2/h^3.$$

Because the same collision integral provides the lowest-order approximation to the thermal conductivity, the ratio of the two transport coefficients is, to this first approximation, independent of the scattering law:

$$(m/k)\kappa/\eta = 4,$$

making it possible to estimate values of the heat conductivity from the shear viscosity.

The second approach we have followed replaces the collision-integral analysis with a numerical average over simulated equilibrium collisions. We use Bird's method, selecting pairs of particles for collision with a probability proportional to their relative speed. We consider the Boltzmann equation for a homogeneously sheared system with

$$\partial u_x/\partial y \equiv \dot{\epsilon} \rightarrow dv_x/dt = -\dot{\epsilon}v_y.$$

The first approximation to the nonequilibrium part of the distribution function for $\{v_x, v_y\}$ is proportional to $f_{\text{EQ}}mv_xv_y/kT$. Multiplying the Boltzmann equation by mv_xv_y/kT and integrating over all velocities links the perturbation to the collision rate Γ_1 and gives a transparent expression for the shear viscosity:

$$\eta = P/\omega, \quad \omega = \Gamma_1 \langle \delta^2 \rangle_{\text{EQ}}, \quad \Gamma_1 = 2(Nh/V)(\pi kT/m)^{1/2};$$

$$\delta \equiv [(mv_xv_y) - (mv_xv_y)' + (mv_xv_y)_1 - (mv_xv_y)'_1]/2kT.$$

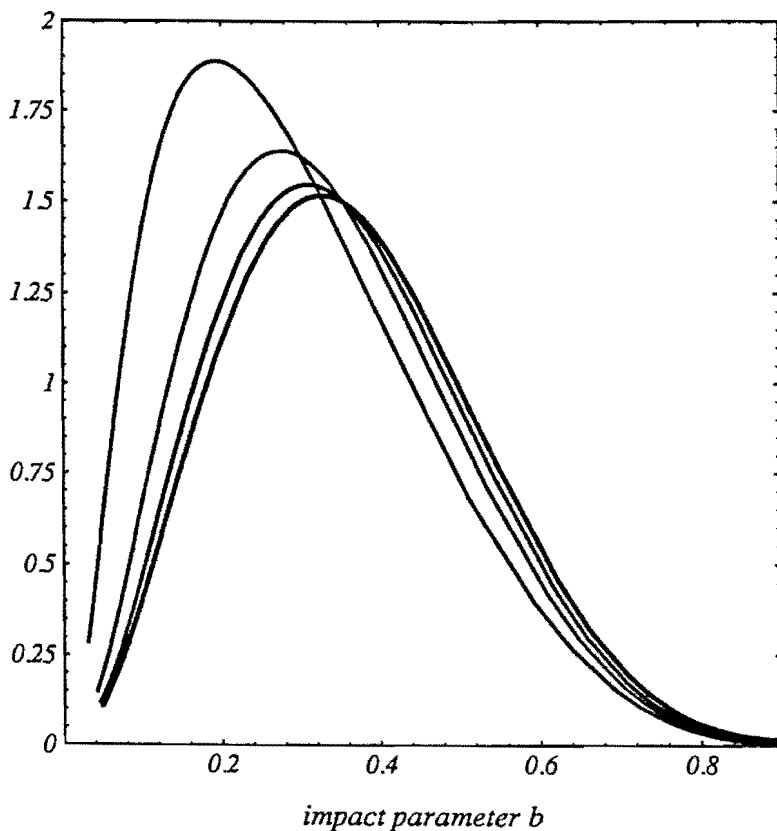


Fig. 2. Dependence of the scattering angle χ on the center-of-mass energy E and impact parameter b for Lucy's potential. The curves plotted show $E^2 \sin^2 \chi$, corresponding (from top to bottom) to energies of 2.5, 5.0, 10, and 20. Note the approach to the high-temperature limiting law, $\chi^2 \propto 1/T^2$.

Γ_1 is the collision rate per particle and δ is a symmetrized change in the shear stress contribution of two colliding particles, with its square averaged over a chain of equilibrium collisions. At low temperature this formula reproduces the first approximation to the low-density hard-disk shear viscosity cited by Gass [13], and at high temperature, where scattering is relatively inefficient, it likewise continues to provide a useful numerical evaluation of the viscosity.

The third approach, and the simplest of them all, also makes use of Bird's statistical method for solving the Boltzmann equation by generating stochastic collisions, but applied to a nonequilibrium system undergoing homogeneous shear flow. Each time step Δt of the nonequilibrium simulation proceeds in three stages: (i) first, all particles undergo a velocity change due to shear:

$$\Delta v_x = -v_y \dot{\epsilon} \Delta t,$$

with the velocities $\{v_x, v_y\}$ being relative velocities, measured relative to the local stream velocity $(u_x, 0)$; (ii) next, all these velocities are scaled, to maintain the kinetic energy at the equipartition value, NkT ; (iii) finally, a pair of particles is selected for collision, with the relative probability of each pair proportional to the relative speed of that pair. It is clear that reducing the time step Δt and increasing the number of

particles considered will eventually converge to the solution of Boltzmann equation, as was first pointed out by Bird [15].

Within the numerical accuracy of our work, about 1%, all three methods for determining the shear viscosity agree. Selected values from the last two methods are given in Table 4. The data in Table 4 provide a smooth interpolation between the low-temperature $T^{1/2}$ hard-disk viscosity and the high-temperature weak-scattering dependence, $T^{5/2}$. Fig. 3 shows this interpolation, as well as the good agreement of the data with the analytic form it suggests:

$$\eta_{\text{LUCY}} = [0.24(mkT)^{1/2}/h] + [0.94(mkT)^{1/2}(kTh^2)^2/h].$$

The viscosities from this interpolation formula are very close to those from the present direct low-density simulations. They also provide a useful rough estimate for viscosities at high temperature and high density. A high-density, relatively high-temperature simulation with the Lucy potential [3] gave a shear viscosity of 13, while the above interpolation formula provides the estimate 5.5. Thus the Enskog theory, which suggests that the low-density form be used unchanged at high density, can be in error by as much as a factor of two.

There have been no computer simulations for the heat conductivity, using Lucy's potential. The Evans–Gillan approach [16,17] to homogeneous field-driven heat

Table 4
Shear viscosity for the Lucy potential,

$$\phi_{\text{LUCY}} \equiv (5/\pi h^2)[1 - 6(r/h)^2 + 8(r/h)^3 - 3(r/h)^4],$$

at low density, and with $m = k = h = 1$, as a function of temperature T . Viscosities for other values of the range h can be estimated by using the scaling relationship derived in the text. The heat conductivity κ can be estimated by using Sengers' result, as quoted by Gass [13], $\kappa = 4\eta k/m$. The entries shown in the table were computed in two independent ways, solving the Boltzmann equation, using Bird's method with 100 particles, and evaluating the equilibrium collisionally averaged shear-stress fluctuation. The strain rates $\dot{\epsilon}$ given in the table refer to simulations with 2 000 000 Runge–Kutta time steps ($\Delta t = 0.01$) calculated using Bird's approach. The single-particle collision rate Γ_1 was chosen such that one collision occurred during each Runge–Kutta time step. The data in the table are taken from the last half of each simulation. At high temperatures where thermal scattering is very inefficient, this method becomes impractical. Thus no data were obtained for temperatures higher than 10. The kinetic-theory approach is less severely limited at high temperature. Those results, based on equilibrium averages over 100 000 collisions, at zero strain rate, are somewhat more accurate than the nonequilibrium results, and appear in the final column. We have also confirmed the kinetic-theory calculation at selected temperatures by making direct evaluations of the corresponding collision integral

T	$2\dot{\epsilon}\Gamma_1$	η_{NONEQ}	η_{EQ}
0.01	0.2000	0.0296	0.030
0.03	0.1000	0.054	0.053
0.10	0.0500	0.105	0.105
0.30	0.0300	0.22	0.211
1.00	0.0100	1.3	1.20
3.00	0.0010	12	14.1
10.00	0.0001	300	290

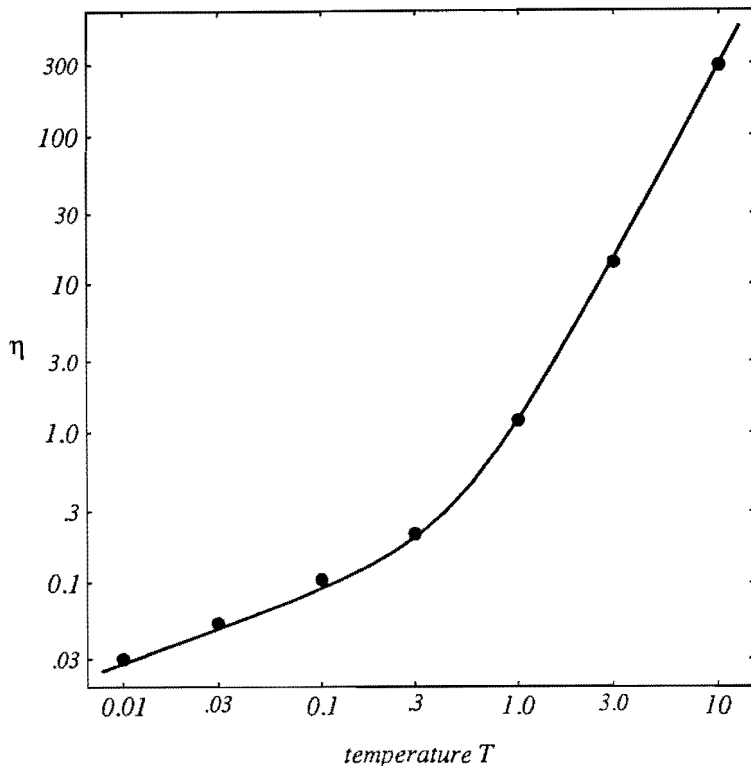


Fig. 3. Temperature dependence of the viscosity for Lucy's potential. The smooth curve (plotted for m , k , and h all equal to unity) is the sum of the high- and low-temperature limits discussed in the text:

$$\eta \approx \eta_{\text{FIT}} \equiv 0.24(mkT)^{1/2}/h + 0.94(mkT)^{1/2}(k\sqrt{h^2})^2/h.$$

currents seems to fail in two dimensions, necessitating the study of an inhomogeneous flow driven by heat reservoirs, as in [12].

At low density the Boltzmann equation establishes the ratio of conductivity to viscosity. The Chapman–Enskog approach to solving the Boltzmann equation establishes that, to lowest order, both the viscosity and the heat conductivity are given by the same collision integral. Thus Sengers' ratio of the transport coefficients for disks, as quoted by Gass [13], should apply also to other potentials, such as Lucy's. This reasoning also suggests that the transport coefficients predicted by the approximate Krook–Boltzmann and Fokker–Planck equations have substantial errors. For the transport coefficient ratio, the correct, Krook–Boltzmann, and Fokker–Planck results for a two-dimensional gas are as follows:

$$(m/k)(\kappa/\eta) = \{4, 2, \frac{4}{3}\}.$$

This dimensionless ratio of transport coefficients is independent of the relaxation times $\{\tau_{\text{KB}}, \tau_{\text{FP}}\}$ which occur in the two approximate kinetic equations:

$$(df/dt)_{\text{KB}} = [f_{\text{EQ}} - f]/\tau_{\text{KB}},$$

$$(df/dt)_{\text{FP}} = (mkT/\tau_{\text{FP}})\nabla_p^2 f + (1/\tau_{\text{FP}})\nabla_p(fp),$$

$$\eta_{\text{KB}} = P\tau_{\text{KB}}, \quad \kappa_{\text{KB}} = 2P(k/m)\tau_{\text{KB}};$$

$$\eta_{\text{FP}} = \frac{1}{2}P\tau_{\text{FP}}, \quad \kappa_{\text{FP}} = \frac{2}{3}P(k/m)\tau_{\text{FP}}.$$

In all these expressions k is Boltzmann's constant and m is the particle mass. Note that the differential operators on the right-hand side of the Fokker–Planck equation represent derivatives ∇_p with respect to the momentum p .

The disagreement between the exact Boltzmann equation and the Fokker–Planck equation might seem surprising in view of the common belief that the Boltzmann equation reduces to the Fokker–Planck equation in the weak-scattering (high-temperature) limit. An investigation of the usefulness of the Fokker–Planck equation for weak scattering would help to dispel this confusion. A theory specially suited to the study of weak interactions was developed by Rainwater and Hess [18]. The nonlinear aspects of transport are of particular interest, and are certainly well within the capabilities of computer simulation [19]. A study of two-dimensional shock waves following up the exploratory calculations presented in Kum's thesis [5] would be relevant and interesting. The present data suggest that twofold shock compression of a quiescent ideal gas would generate an "artificial viscosity" (that is, a viscosity characterizing the Lucy potential) of order unity, resulting in a shock width only a few times greater than the range of the weight function.

6. Summary and conclusions

The thermomechanical and transport properties using Lucy's potential are not only relatively simple, but can also be relatively simply understood on the basis of high-temperature high-density perturbation theory. By using these ideas, in conjunction with the principle of corresponding states, it is possible to estimate the numerical impact of the intrinsic Lucy-potential viscosity on fluid-phase simulations of Navier–Stokes solutions.

Such estimates need to take both thermal and size effects into account. Thermal effects require a kinetic temperature estimate. This is not an easy matter. An estimate can be based on comparing the two velocities which characterize each smooth particle: the individual particle velocity v_i , and the collective hydrodynamic velocity $\langle v \rangle$ at the particle location. This difference can be estimated in at least two ways. On the basis of a Taylor series expansion of the hydrodynamic velocity, the velocity difference would vary as $h^2 \nabla^2 \langle v \rangle$. Alternatively, the relative particle velocities might instead be of order c , where c is the sound speed. Because the viscosity depends upon the local temperature as $T^{5/2} \propto c^{5/2}$, with an additional dependence on h of order $h^{1+(3D/2)}$ in D dimensions, either estimate suggests a very strong dependence of flow simulations on h . Such effects dominate the true viscosity in some situations and suggest a sharp threshold for the applicability of smooth particle methods to fluid flow problems, with the quality of approximation depending very strongly on the number of particles used.

In Kum's two-dimensional Rayleigh–Bénard simulations with only 500 smooth particles, for example, a fourfold increase in the Rayleigh number ostensibly driving the convective flow produced no noticeable change whatever. A 5000-particle model

of the same flow behaved properly. In certain circumstances, discussed fully in connection with Kum's work, the repulsive forces of the smooth particle weighting functions can even cause freezing of the flow. This sensitivity of flows with only a few degrees of freedom to the form of the weighting function is readily understandable on the basis of the analysis in the present work. It appears that the maximum tractable Reynolds number increases very rapidly with the number of particles, more rapidly than $N^{3/2}$, and thus more rapidly than the $N^{1+(1/D)}$ dependence of the computational work. Accordingly, we conclude that applications of the smooth particle method to complex flows deserve continued vigorous investigation.

Acknowledgements

A part of this work was carried out during a visit of WGH to the Technical University of Berlin in the winter of 1995–1996. Discussions with Carol Hoover, Oyeon Kum, and Harald Posch helped to motivate this effort. Work at the Lawrence Livermore National Laboratory was supported by University of California Contract W-7405-Eng-48.

References

- [1] J.J. Monaghan, *Ann. Rev. Astron. Astrophys.* 30 (1992) 543.
- [2] H.E. Trease, M.J. Fritts and W.P. Crowley, eds., *Advances in the Free-Lagrange Method, Lecture Notes in Physics*, Vol. 395 (Springer, Berlin, 1991).
- [3] H.A. Posch, W.G. Hoover and O. Kum, *Phys. Rev. E* 52 (1995) 1711.
- [4] O. Kum, W.G. Hoover and H.A. Posch, *Phys. Rev. E* 52 (1995) 4899.
- [5] O. Kum, Nonequilibrium flows using smooth particle applied mechanics, Ph. D. Thesis, University of California at Davis/Livermore (1995).
- [6] J.O. Hirschfelder, C.F. Curtiss and R.B. Bird, *Molecular Theory of Gases and Liquids* (Wiley, New York, 1954).
- [7] O. Kum and W.G. Hoover, *J. Stat. Phys.* 76 (1994) 1075.
- [8] W.G. Hoover, A.C. Holt and D.R. Squire, *Physica* 42 (1969) 388; 44 (1969) 437.
- [9] W.G. Hoover, *Computational Statistical Mechanics* (Elsevier, Amsterdam, 1991).
- [10] W.G. Hoover, *Phys. Lett. A* 204 (1995) 133.
- [11] W.G. Hoover and H.A. Posch, *Phys. Rev. E* 51 (1995) 273.
- [12] D. Risso and P. Cordero, *J. Stat. Phys.* 82 (1996) 1453.
- [13] D.M. Gass, *J. Chem. Phys.* 54 (1971) 1898.
- [14] G. Schmidt, W.E. Koehler and S. Hess, *Z. Naturforsch. A* 36 (1981) 545.
- [15] See the articles by G.A. Bird and A.L. Garcia, in: *Microscopic Simulations of Complex Flows*, ed. M. Mareschal (Plenum, New York, 1990).
- [16] D.J. Evans, *Phys. Lett. A* 91 (1982) 457.
- [17] M.J. Gillan, *J. Phys. C* 16 (1983) 869.
- [18] J.C. Rainwater and S. Hess, *Physica A* 118 (1983) 371.
- [19] W. Loose and S. Hess, *Phys. Rev. A* 37 (1988) 2099.